Heliyon 9 (2023) e19402

Contents lists available at ScienceDirect

Heliyon

journal homepage: www.cell.com/heliyon

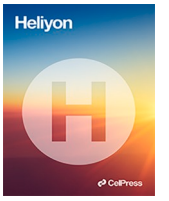

Investigating of transition state on the Pd–Au decorated ZnO nanoparticle layers for gas sensor application

Niyom Hongsith [a,c,*], Suphansa Chansuriya [a], Sakda Koenrobket [a], Somrit Unai [a], Ekasiddh Wongrat [a,c], Anurak Prasatkhetragarn [b,c]

[a] Department of Physics, School of Science, University of Phayao, Phayao, 56000, Thailand
[b] Department of Material Science, School of Science, University of Phayao, Phayao, 56000, Thailand
[c] Unit of Excellence on Advanced Materials for Sensors, University of Phayao, Phayao, 56000, Thailand

ARTICLE INFO

Keywords:
Near-IR spectroscopy
Zeta potential
ZnO
Nanostructure
Gas sensor

ABSTRACT

In this work, the mechanism of the transition state of electron transfer reaction on the surface of the ZnO nanoparticles-based gas sensor has been investigated. The deposited ZnO nanoparticles thick films on glass slides had been synthesized by the current heating method and modified its surface by coating novel metals of gold and palladium with a sputtering technique with different sputtering times of 45–180 s. Field emission electron microscopy (FE-SEM), x-ray diffraction spectroscopy (XRD), and energy dispersive spectroscopy (EDS) were used for the characterization of ZnO nanoparticle thick films. After that, the reflectance spectra of films were investigated using Near-IR spectroscopy in the range of 900–2500 nm to study the surface absorption efficiency. The decrease in reflectance spectra was observed for conditions over 90 s of sputtering time. The particle size distribution and zeta potential of ZnO nanoparticles were analyzed using the dynamic light scattering technique for the calculation of particle size and the electrical charge potential. The results showed that the size particle distribution ranged from 155 to 245 nm and the more extensive range of 360–1100 nm. The optimized zeta potential of −14.44 mV was exhibited at the sputtering time of 45 s. Finally, the gas sensing mechanism in terms of surface charge density was proposed and used to explain the sensitivity enhancement of both resistive and capacitive gas sensors.

1. Introduction

ZnO nanostructure is an attractive material widely used for gas sensor applications. Because the gas sensor based on nanostructure usually exhibits high to ultrahigh sensitivity in the range of 100–1000 times [1–5]. The various nanostructure of ZnO-based gas sensors has been continually reported, such as nanowire, nanobelts, nanoparticles or nanotetrapods, etc. [6–9]. In general, the assessment of gas sensor performance entails the determination of sensitivity, denoted as S, which is derived from the ratio of the material's electrical properties in both a normal atmospheric environment and a gas atmosphere.

From previous work [10,11], the gas sensing mechanism of ZnO gas sensing has been clearly explained in terms of the charge activity, such as O– O^{2-}, H^{+}, or OH^{-} on the surface of the material. This activity is strongly depending on the operating temperature of ZnO. The optimum temperature for the ZnO-based gas sensor is about 250–350 °C, which exhibits the highest sensitivity. At high

* Corresponding author. Department of Physics, School of Science, University of Phayao, Phayao, 56000, Thailand.
E-mail address: niyom.ho@up.ac.th (N. Hongsith).

https://doi.org/10.1016/j.heliyon.2023.e19402
Received 19 April 2023; Received in revised form 21 August 2023; Accepted 22 August 2023
Available online 25 August 2023
2405-8440/© 2023 Published by Elsevier Ltd. This is an open access article under the CC BY-NC-ND license (http://creativecommons.org/licenses/by-nc-nd/4.0/).

temperatures, the oxygen molecules in the normal atmosphere are adsorbed on the surface of ZnO and then form an oxygen ion by attracting electrons from the ZnO. These oxygen ions are excited to react with the target gas molecule and give up the electron to the surface.

Investigating the transition state of electron transfer reaction on the surface of the ZnO gas sensor during an on-off state of gas activated can be observed by measuring the changing of the electrical property. First, the resistive type ZnO gas sensor is monitored by measuring the sensor's resistance. For example, the resistance of ZnO rapidly decreased in ethanol or acetone atmosphere, and the sensitivity was defined as the ratio of resistivity in air and gas ambiance. Second, on the other hand, the capacitive type ZnO gas sensor is monitored by measuring the sensor's capacitance. Likewise, in ethanol and acetone atmosphere, the capacitance of the sensor increased when gas was injected into the sensor. It was different from the resistive-type gas sensor. These mechanisms are still a subject of discussion [9–12].

However, the sensitivity enhancement of the ZnO gas sensor has been widely reported. One technique is a modified surface method by adding noble metals such as Au, Pt, Pd, or Ag on the ZnO surface using various techniques, whether solution drop method or sputtering, etc. [4,13–19]. Especially sputtering is one such method commonly used for depositing thin films. In sputtering, atoms or ions from a target material are ejected and deposited onto a substrate surface under the influence of a high-energy plasma. It is a very efficient coating, with a minimal amount of substance used in each coating, which will reduce the cost of the application. The metal on the surface can act as a catalyst to enhance charge activity on the surface of ZnO and improve sensor sensitivity. In the nanometer scale, the surface-to-volume ratio is a critical parameter. It is related to the density of charge activity on the surface. However, the sensing mechanism of the sensor could explain a parameter of the surface charge density. The sensor's sensitivity in terms of surface charge density has been proposed [11].

In this work, ZnO nanoparticles were deposited onto a glass slide substrate using the current heating method, and novel metals of Au:Pd particles were added onto its surface through a sputtering technique with different time conditions. Effect of Au:Pd particles on the surface of ZnO nanoparticles, morphologies, crystal structure, atomic composition, and optical properties were investigated and discussed. After that, the particle size distribution and zeta potential of ZnO nanoparticles were analyzed. Finally, the gas sensing mechanism in terms of surface charge density was proposed and used to explain the sensitivity enhancement of both resistive and capacitive gas sensors.

2. Materials and methods

2.1. Preparation of ZnO nanoparticles films by current heating method

The synthesis of ZnO nanostructured films on a glass substrate was accomplished by utilizing the current heating technique. A cylindrical shape of pure Zn, with dimensions of 6 mm in diameter and 10 mm in height, was fabricated through the compression of 99.99% pure zinc powder and a polyvinyl alcohol (PVA) solution with a concentration of 1% by weight. Subsequently, the resulting rod was subjected to heating at 400 °C for a duration of 3 h. The experimental setup for the preparation of ZnO products involved the use of a conducting metal electrode, which made contact with both ends of the Zn rod. The configuration of the preparation setup is depicted in Fig. 1 (a). Subsequently, a direct current of 20A was applied to the zinc rod, activating the gas plasma. As a consequence of the rapid thermal oxidation of zinc under an air atmosphere [4], white fog was generated within the chamber. A glass slide substrate was placed at a distance of approximately 5 cm from the heating rod, as illustrated in Fig. 1 (b), to directly collect the ZnO products from the plasma.

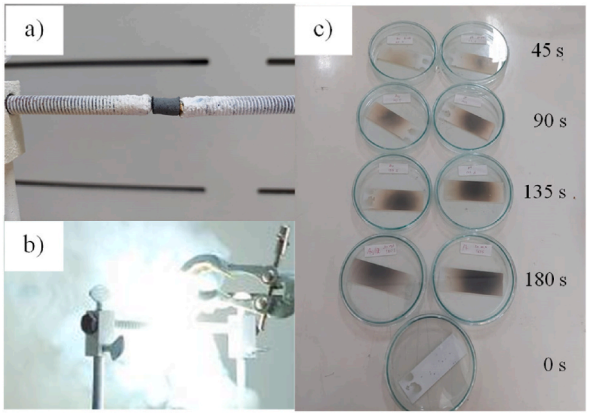

Fig. 1. Synthesis of ZnO nanoparticles, (a) Zn rod with eletrodes (b) plasma activated (c) the surface-modified ZnO nanoparticle films under different conditions with the 45, 90, 135, and 180 s sputtering.

2.2. Pd–Au decorated ZnO particle layers

The surface of ZnO nanostructure films was modified by depositing the novel metal of Pd and Au on the surface by sputtering the SPI-module™ sputter coater. The sputtering process involved setting specific time conditions of 45 s, 90 s, 135 s, and 180 s while maintaining a constant direct current (DC) of 20 mA. The distance between the Pd:Au target and ZnO nanostructure films was approximately 5 cm. Fig. 1 (c) presents the surface-modified ZnO nanoparticle films under different conditions. It was observed that the color of ZnO particle films changed from white to various shades of grey and black, with the intensity of color deepening corresponding to the different sputtering times.

2.3. Characterization of ZnO nanostructures

The surface morphologies and crystal structure of ZnO nanostructures on the substrate were characterized using Field Emission Scanning Electron Microscopy (FE-SEM) and X-Rays Diffractometry (XRD). The presence of gold and palladium nanoparticles on the surface of the ZnO nanostructure was observed by energy dispersive spectroscopy (EDS). The analysis of particle size distribution and zeta potential of ZnO nanostructures were analyzed by using dynamic light scattering technique with a Zeta-potential & Particle size Analyzer ELSZ-2000 series. To separate the ZnO nanostructures from the substrate, they were dissolved in distilled water and subjected to sonication for 2 min. The pH value of the solution was adjusted to 7, and the resulting pattern, featuring the distributions of sizes and zeta potential, was recorded. Finally, the Near-IR spectra of the films, within the range of 900–2500 nm, were measured under conditions of both room and high temperature in the presence of ethanol and acetone atmosphere.

3. Results and discussion

3.1. Characterization of ZnO nanoparticles and surface-modified ZnO nanoparticles

The thick films on the glass substrate, under the condition of 0 s, exhibited white color, as depicted in Fig. 1 (c). It was suggested that the transformation of metallic zinc into ZnO occurred via an oxidation reaction. The thickness of thick films measured approximately 56 μm, as shown in the cross-section image represented in Fig. 2 (a). Moreover, Fig. 2 (b) displayed a high-resolution FE-SEM image from a top-view perspective, revealing the observation of nanostructured ZnO films on the glass substrate. Subsequently, Fig. 2 (c)–(f) displayed the surface-modified ZnO nanostructures, corresponding to sputtering time conditions of 40 s, 90 s, 135 s, and 180 s, respectively. The results suggested that significant changes in the surface morphologies of ZnO nanostructured films were observed. Furthermore, it was confirmed that the ZnO films were coated with Au and Pd metal, corroborating the findings from the optical image shown in Fig. 1 (c).

Fig. 3 (a) displays the size distribution of ZnO products, revealing two distinct ranges of sizes. The smaller diameter products

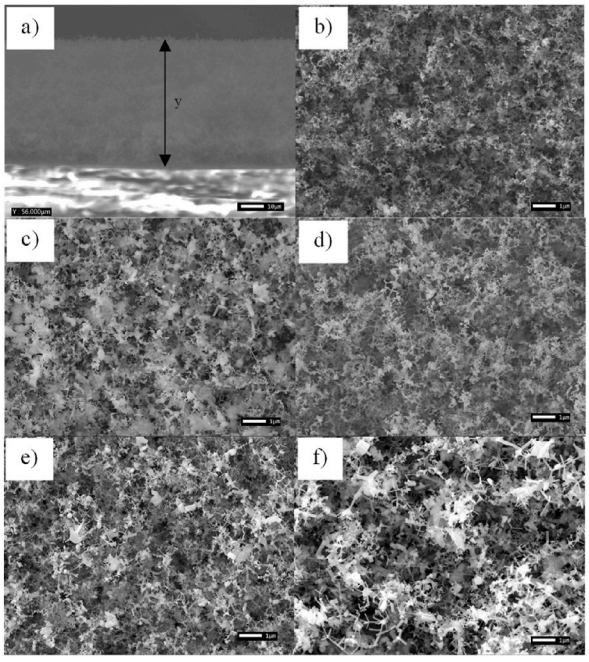

Fig. 2. FE-SEM image of (a) the thickness of ZnO nanostructures layer, (b) ZnO, (c)–(f) Pd–Au decorated ZnO particle layers with 45 s, 90 s, 135 s and 180 s sputtering time, respectively.

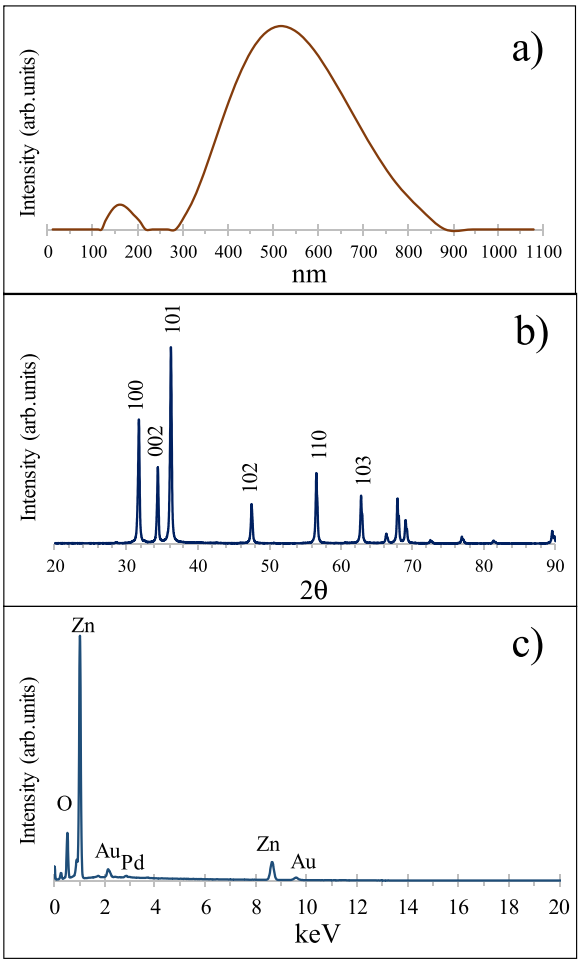

Fig. 3. (a) Size distribution of ZnO nanoparticles and (b) XRD pattern of ZnO nanoparticles films and (c) EDS spectra of Pd–Au decorated ZnO particle layers.

exhibited a range of 155–245 nm, while the larger ones showed a broader range of 360–1100 nm. Fig. 3 (b) shows the XRD pattern of the nanoparticles prepared on a glass substrate. The XRD spectra exhibit diffraction peaks corresponding to a hexagonal ZnO structure, characterized by lattice constants of a = 3.240 Å and c = 5.196 Å. The absence of peaks from Zn or other phases suggests that the product is indeed a ZnO nanoparticle.

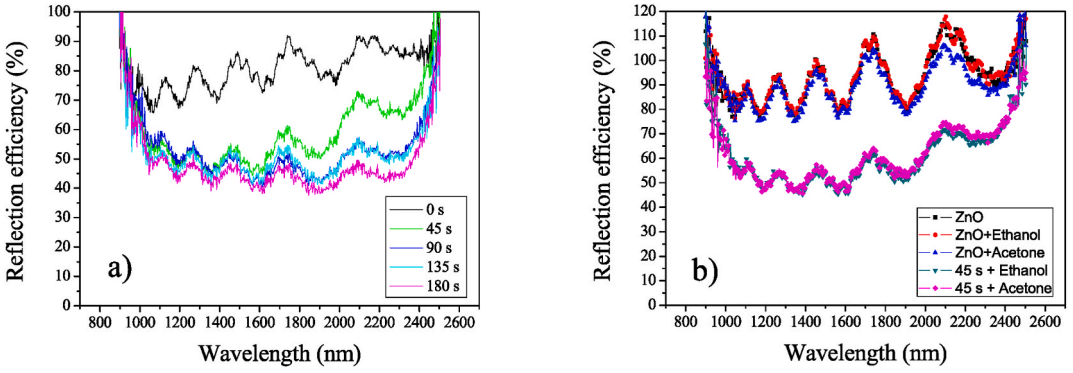

Fig. 4. Near-IR spectra of ZnO nanoparticles films and Pd–Au decorated ZnO particle layers with (a) at 160 °C and (b) with and without ethanol and acetone gas.

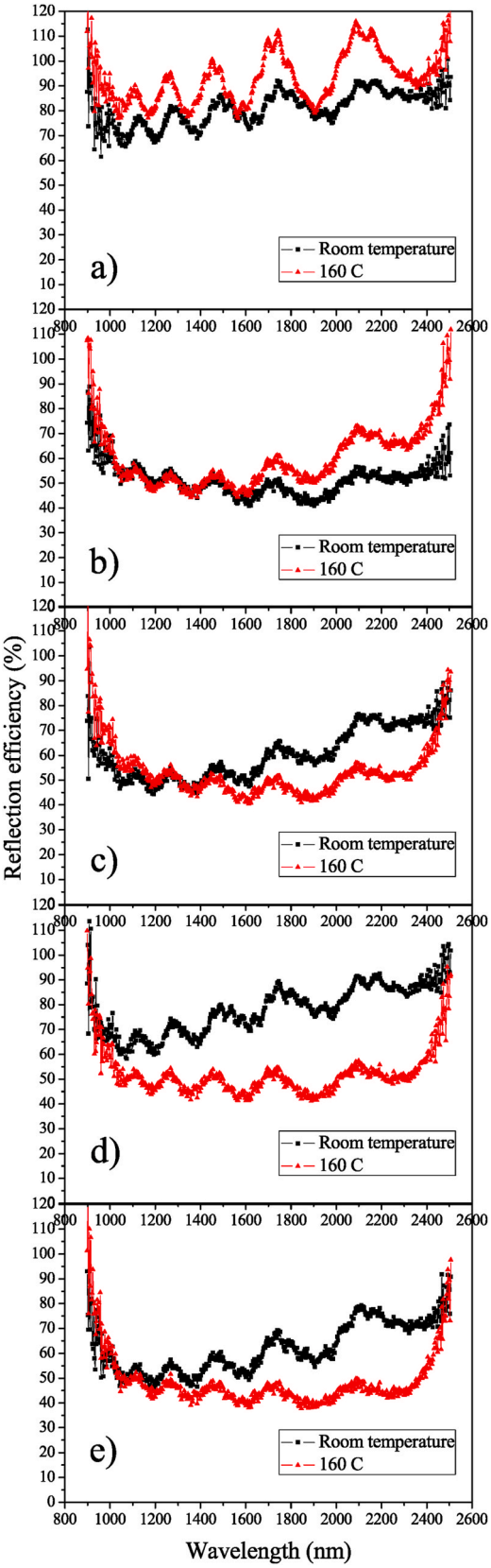

(caption on next page)

Fig. 5. Near-IR spectra of ZnO nanoparticles films and Pd–Au decorated ZnO particle layers campapared between room temperature and 160 °C of (a)–(e) for 0 s, 45 s, 90 s, 135 s, and 180 s sputtering time, respectively.

Fig. 3 (c) shows the EDS spectra of surface-modified ZnO nanostructure thick films by sputtering Au: Pd metal. The presence of peaks corresponding to Au, Zn, O, and Pd is observed in the spectra. The average atomic percent is a linear relation to the sputtering time, for example, the atomic% of Au is 0.77% and 1.05% for the sputtering time of the 90 s and 180 s, and the atomic% of Pd is 0.27% and 0.34%, respectively. It is noteworthy that, in a previous study [4], the gold amount on the ZnO surface was determined using the Rutherford Backscattering (RBS) technique, which exhibited a linear relationship between Au atom concentration and sputtering time. This finding strongly suggests the presence of varying amounts of metal on the ZnO surface corresponding to different sputtering times.

3.2. Near-IR reflection spectra of surface-modified ZnO nanoparticles

The Near-IR reflection spectra of ZnO and surface-modified ZnO nanostructured films under various conditions were investigated. It was observed that the 180° degree reflection spectra of various films at room temperature were largely similar across all conditions. However, at a high temperature of 160 °C, as shown in Fig. 4 (a), slight decreases in reflectance were evident, with the reflectance efficiency showing an inverse relationship to the sputtering time. This phenomenon was attributed to the increased presence of metal, leading to higher charge density on the ZnO surface. Consequently, this is a clear explanation regarding the increase of charge carrier and temperature effects on semiconducting materials.

In Fig. 4 (b), the reflection spectra of films in ethanol and acetone gas atmospheres were presented. However, the shifting of reflection spectra between the air atmosphere and the gas vapor atmosphere cannot be observed. As a result, this is suggested that light reflection efficiency may not be an effective means for monitoring the surface charge density of the ZnO surface. Comparing the reflectance efficiency at low and high temperatures, as shown in Fig. 5 (a)-(e), it was noted that a decreasing trend in reflectance spectra was evident for sputtering times between 90 s and 180 s. It was further suggested that the optimal metal adding concentrations were found within the range of 0–45 s sputtering time. However, the relation between sensitivity and sputtering time has been reported

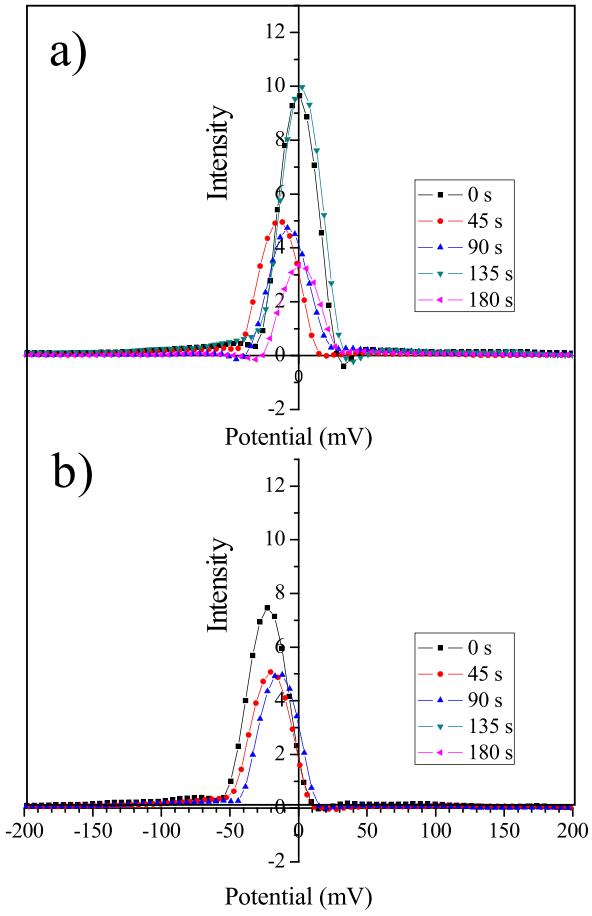

Fig. 6. Zeta potential of ZnO nanoparticles and Pd–Au decorated ZnO particle layers with (a) and (b) with ethanol and acetone solution.

in previous research [4]. The highest value of sensitivity was achieved at 60 s of sputtering time condition. It is evident that the sensor response increased at short sputtering times, reaching its maximum value at 60 s, and then decreased for longer sputtering times.

3.3. Zeta potential analysis

The surface charge density of particles can be determined using the Zeta potential analyzer. Although zeta potential is an electrical property that indicates the stability of colloidal dispersions, it can be applied to calculate the particle's surface charge. Fig. 6 (a) shows the zeta potential of ZnO and surface-modified ZnO nanoparticles. The results showed that the particle's zeta potential strongly depends on the sputtering time. An optimized zeta potential of −14.44 mV was observed at a sputtering time of 45 s, and this condition was suggested to exhibit optimized sensitivity. Interestingly, the enhancement of the sensitivity of the ZnO gas sensor by adding Au metal exhibited a maximum value of 478 at the sputtering time of approximately 60 s and then decreased at a longer sputtering time [4].

Furthermore, the zeta potential of the particle under the condition of 45s sputtering time was recalculated by employing ethanol and acetone as the solvent solution. The zeta potential curves, depicted in Fig. 6 (b), exhibited a slight increase, providing support for the presence of activity on the ZnO surface. The summarized data on the zeta potential of both ZnO and surface-modified ZnO nanoparticles are presented in Table 1 and Table 2, respectively.

3.4. Sensing mechanism via electron surface charge density

Generally, ZnO is typically classified as an n-type metal oxide semiconductor and is extensively utilized in resistive-type gas sensors. The resistance of the ZnO gas sensor exhibits a decreasing trend with increasing operating temperature due to the increase of electron carriers in the conduction band by absorbing the thermal energy. In the presence of an oxygen ambience, these electrons are extracted by the adsorbed oxygen ions, *O*- or *O2*-, leading to an increase in the resistance of the ZnO sensor due to the reduction in carrier concentration [9]. However, when the ZnO gas sensor operates in a target gas ambiance, particularly in the presence of reducing gases like ethanol and acetone, the electrons generated through chemical reactions are subsequently reintegrated into the conduction band, leading to a decrease in sensor resistance.

Similarly, in the case of capacitive-type sensors, the capacitance of the ZnO sensor exhibited an increase with the rise in operating temperature [12]. It was suggested that the adsorbed oxygen ions on the sensor surface act as the electrical dipole moment and reduce the electrical field within the material and leading to an increase in capacitance.

The evidence of this hypothesis was confirmed through the investigation of the relationship between sensor capacitance and temperature in air ambiance, as shown in Fig. 7 (a). The capacitance of the sensor was highly increased when the temperature started at 250 °C due to the thermal condition of adsorbed oxygen ions. However, the capacitance was not significantly changed, and the signal was unstable when removing oxygen from the chamber. Besides, the resistance of the sensor was increased by consideration of the phase angle change in function of the temperature, as shown in the inset picture in Fig. 7 (b).

In ethanal and acetone ambiance, the capacitance of the ZnO sensor was increased when injecting the gas vapor into the chamber. This phenomenon is amazing because it is different from the resistive-type gas sensor. Furthermore, the sensor's sensitivity was found to be dependent on several factors, including gas concentration, operating temperature, and gas species. Thus, to explain the capacitive-type gas sensing characteristics, the utilization of the surface charge density parameter appears to be a viable approach. Consequently, in order to elucidate the underlying mechanism, the explanation has been categorized into two distinct sensing states.

3.5. The gas sensing mechanism of capacitive-type gas sensor

3.5.1. State I-steady state

This state corresponds to the condition in which the sensor operates within an oxygen ambiance at a high temperature. In this state, adsorbed oxygen ions, which refer to *O*- or *O2*- are distributed on the surface of the sensor.

3.5.2. State II-gas active state

From a previous report [10,11], it was suggested that the resistance of the sensor is contributed from two parts, including the resistance along individual a nanoparticle and the resistance between nanoparticles. In the context of a capacitive-type gas sensor, the surface depletion layer between nanoparticles was considered. The presence of this adsorbed layer introduces additional electric charges, leading to a modification in the electrical field distribution within the material. Consequently, the effective electric field,

Table 1
Zeta potential and some physical properties of ZnO and Pd–Au decorated ZnO nanoparticle layers.

	Mobility (cm^2/Vs)	Zeta Potential (mV)	Electric Field (V/cm)
ZnO	−2.93E-06	−0.38	−12.13
ZnO + Au:Pd45s	−1.13E-04	−14.44	−12.14
ZnO + Au:Pd90s	−5.58E-05	−7.16	12.21
ZnO + Au:Pd135s	1.46E-05	1.88	−12.21
ZnO + Au:Pd180s	1.20E-05	1.53	12.29

Table 2
Zeta potential and some physical properties of ZnO and surface-modified ZnO nanoparticles with ethanol and acetone solution.

	Mobility (cm^2/Vs)	Zeta Potential (mV)	Electric Field (V/cm)
ZnO + Au:Pd45s	−1.13E-04	−14.44	−12.14
ZnO + Au:Pd45s + Ethanol	−1.76E-04	−22.51	−12.21
ZnO + Au:Pd45s + Acetone	−1.56E-04	−20.14	−12.21

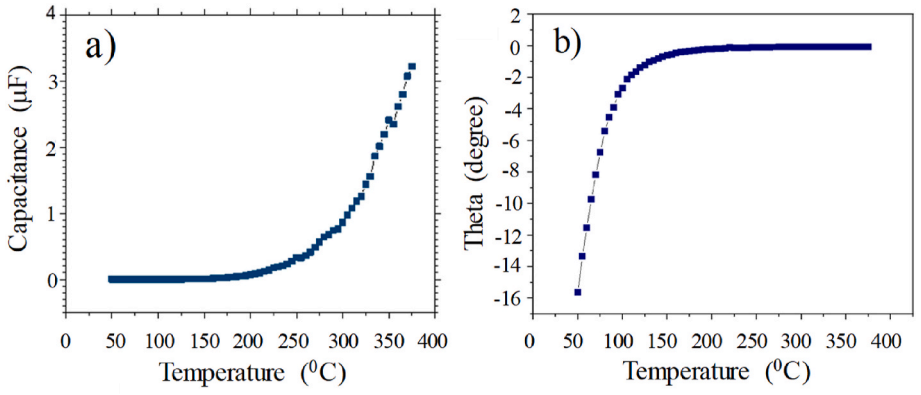

Fig. 7. (a) The relationship between capacitance of sensor and temperature in air ambiance and (b) the phase angle change in function of temperature.

$E_{effective}$, between the electrodes is reduced, resulting in an increase in capacitance. The presence of the dielectric decreases the electric field produced by a given charge density, σ, could be described as follow in equation (1).

$$E_{effective} = \frac{\sigma}{\varepsilon} \tag{1}$$

However, according to the depletion layer or the space charge model, L_d (Debye length) can be expressed by as follow in equation (2) [10,20–22].

$$L_d = \left(\frac{\varepsilon k_B T}{q^2 n}\right)^{1/2} \tag{2}$$

where ε is a static dielectric constant, q is an electrical charge of a carrier, and n is a carrier concentration in the conduction band. So, the Debye length is influenced by two key parameters: the carrier concentration and the dielectric constant, both considered at a steady operating temperature. At an optimized operating temperature, oxygen ions become adsorbed by attaching an electron to the surface of the particle. Consequently, a depletion layer is formed on the surface of the particle with an initial thickness. Subsequently, when the sensor is exposed to a reducing gas, it reacts with the oxygen ions present on the surface, resulting in the return of electrons to the material sensor and subsequently reducing the width of the depletion layer. When the gas molecules, such as ethanol and acetone, come into contact with the surface of the ZnO sensor, they are adsorbed onto the sensor's surface. This results in a change in the electrical properties of the ZnO nanostructures, particularly the capacitance.

Upon analyzing the experimental results, it was observed that the properties of surface-modified ZnO nanoparticles exhibited noticeable changes. Both the Near-IR spectroscopy and Zeta potential analyses revealed distinct surface conditions that were dependent on the sputtering time. The presence of metal on the ZnO surface served as a catalyst, enhancing the charge activity on the surface. The detection mechanism of a capacitive-type gas sensor was elucidated, employing the depletion layer and surface charge density. Notably, the capacitance was found to be influenced by several parameters, including the electrode area and the distance between the electrodes, along with the relative permittivity. However, the results of this experiment demonstrated that the capacitance primarily relies on relative permittivity alone.

4. Conclusions

The ZnO nanoparticles have been successfully synthesized by the current heating technique. The size distribution of nanoparticles was about a few hundred nanometers. The surface charge density depends on the sputtering time condition. The reflectance was slightly decreased related to the sputtering time. It is due to the high charge density at the ZnO surface. The optimized zeta potential was exhibited at the sputtering time of 45s. Finally, the gas sensing mechanism in terms of surface charge density was proposed and used to explain the sensitivity enhancement of both resistive and capacitive gas sensors. To illustrate the capacitive-type gas sensing characteristics, two sensing states of the surface charge density parameter could be applied to explain this mechanism. First, the

adsorbed oxygen ions, which refer to as O^- or O^{2-} were distributed on the surface of a sensor at high temperature, and second, when exposed to the reducing gas, it reacted with oxygen ions on the surface and gave back electrons to MOS sensors, decreasing the depletion layer width.

Author contribution statement

Niyom Hongsith: Conceived and designed the experiments; Performed the experiments; Analyzed and interpreted the data; Contributed reagents, materials, analysis tools or data; Wrote the paper.

Suphansa Chansuriya; Sakda Koenrobket: Performed the experiments; Wrote the paper.

Somrit Unai: Conceived and designed the experiments; Analyzed and interpreted the data; Wrote the paper.

Ekasiddh Wongrat; Anurak Prasatkhetragarn: Conceived and designed the experiments; Wrote the paper

Data availability

Data will be made available on request.

Declaration of competing interest

The authors declare that they have no known competing financial interests or personal relationships that could have appeared to influence the work reported in this paper.

Acknowledgments

This research project was supported by the Thailand science research and innovation fund and the University of Phayao, Thailand (Grant No. FF65-RIM071). Niyom Hongsith acknowledge financial support from School of Science University of Phayao, Thailand (Grant No. PBTSC65003).

References

[1] X. Pan, X. Zhao, Ultra-high sensitivity zinc oxide nanocombs for on-chip room temperature carbon monoxide sensing, Sensors 15 (4) (2015) 8919–8930.
[2] C. Li, L. Li, Z. Du, H. Yu, Y. Xiang, Y. Li, Y. Cai, T. Wang, Rapid and ultrahigh ethanol sensing based on Au-coated ZnO nanorods, Nanotechnology 19 (2008), 035501.
[3] V.S. Bhati, M. Hojamberdiev, M. Kumar, Enhanced sensing performance of ZnO nanostructures-based gas sensors: a review, Energy Rep. 6 (2020) 46–62.
[4] E. Wongrat, N. Chanlek, C. Chueaiarrom, B. Samransuksamer, N. Hongsith, S. Choopun, Low temperature ethanol response enhancement of ZnO nanostructures sensor decorated with gold nanoparticles exposed to UV illumination, Sens. Actuators, A 251 (2016) 188–197.
[5] S.K. Min, H. Kim, Y. Noh, K.S. Choi, S.P. Chang, Fabrication of highly sensitive and selective acetone sensor using (p)-Co3O4 nanoparticle-decorated (n)-ZnO nanowires, Thin Solid Films 714 (2020), 138249.
[6] S. Bhatia, N. Verma, R.K. Bedi, Ethanol gas sensor based upon ZnO nanoparticles prepared by different techniques Results, Phys 7 (2017) 801–806.
[7] D. Navas, A. Ibanez, I. Gonzalez, J.L. Palma, P. Dreyse, Controlled dispersion of ZnO nanoparticles produced by basic precipitation in solvothermal processes, Heliyon 6 (2020), e05821.
[8] R. Sha, A. Basak, P.C. Maity, S. Badhulika, ZnO nano-structured based devices for chemical and optical sensing applications, Sens. Actuators Reports 4 (2022), 100098.
[9] A. Mariane, a Franco, P. b Patrick, c Conti, S. Rafaela, a Andre, Daniel S. Correa, A review on chemiresistive ZnO gas sensors, Sens. Actuators Reports 4 (2022), 100100.
[10] N. Hongsith, E. Wongrat, T. Kerdcharoen, S. Choopun, Sensor response formula for sensor based on ZnO nanostructures, Sensor. Actuator. B Chem. 144 (2010) 67–72.
[11] E. Wongrat, N. Hongsith, D. Wongratanaphisan, A. Gardchareon, S. Choopun, Control of depletion layer width via amount of AuNPs for sensor response enhancement in ZnO nanostructure sensor, Sensor. Actuator. B Chem. 181–172 (2012) 230–237.
[12] H.R. Shwetha, S.B. Rudraswamy, A survey on capacitive based CO_2 gas sensor, Inter. J. Eng.Tech. 7 (2018) 918–923.
[13] Y. Nagarjuna, Y.J. Hsiao, Au doping ZnO nanosheets sensing properties of ethanol gas prepared on MEMS device, Coatings 10 (2020) 945.
[14] N. Hongsith, C. Viriyaworasakul, P. Mangkorntong, N. Mangkorntong, S. Choopun, Ethanol sensor based on ZnO and Au-doped ZnO nanowires, Ceram. Int. 34 (2008) 823–826.
[15] P. Cao, Z. Yang, S.T. Navale, S. Han, X. Liu, W. Liu, Y. Lu, F.J. Stadler, D. Zhu, Ethanol sensing behavior of Pd-nanoparticles decorated ZnO-nanorod based chemiresistive gas sensors, Sensor. Actuator. B Chem. 298 (2019), 126850.
[16] R. López, E. Vigueras-Santiago, A.R. Vilchis-Nestor, V.H. Castrejón-Sánchez, M.A. Camacho-López, N. Torres-Gómez, Ether gas-sensor based on Au nanoparticles-decorated ZnO microstructures, Results Phys. 7 (2017) 1818–1823.
[17] R. Sankar-Ganesh, E. Durgadevi, M. Navaneethan, V.L. Patil, S. Ponnusamy, C. Muthamizhchelvan, S. Kawasaki, P.S. Patil, Y. Hayakawa, Low temperature ammonia gas sensor based on Mn-doped ZnO nanoparticle decorated microspheres, J. Alloys Compd. 721 (2017) 182–190.
[18] G. Neri, A. Bonavita, G. Micali, N. Donato, F.A. Deorsola, P. Mossino, I. Amato, B.D. Benedetti, Ethanol sensors based on Pt-doped tin oxide nanopowders synthesised by gel-combustion, Sensor. Actuator. B Chem. 117 (2006) 196–204.
[19] J.R.F. Foronda, L.G. Aryaswara, G.N.C. Santos, S.N.V. Raghu, M.A. Muflikhun, Broad-class volatile organic compounds (VOCs) detection via polyaniline/zinc oxide (PANI/ZnO) composite materials as gas sensor application, Heliyon 9 (2023), e13544.
[20] P. Feng, Q. Wan, T.H. Wang, Contact-controlled sensing properties of flower like ZnO nanostructures, Appl. Phys. Lett. 87 (2005) 213111, 1–3.
[21] Q. Yuan, Y.P. Zhao, L. Li, T. Wang, Ab initio study of ZnO-based gas-sensing mechanisms: surface reconstruction and charge transfer, J. Phys. Chem. C 113 (2009) 6107–6113.
[22] X. Song, Q. Xu, H. Xu, B. Cao, Highly sensitive gold-decorated zinc oxide nanorods sensor for triethylamine working at near room temperature, J. Colloid Interface Sci. 499 (2017) 67–75.